PCCP

Accepted Manuscript

ROYAL SOCIETY OF CHEMISTRY

www.rsc.org/pccp

Why Water Makes 2-Aminopurine Fluorescent

Mario Barbatti [a]* and Hans Lischka [b,c]*

[a] *Max-Planck-Institut für Kohlenforschung, Kaiser-Wilhelm-Platz 1, 45470 Mülheim an der Ruhr, Germany*

[b] *Department of Chemistry and Biochemistry, Texas Tech University, Lubbock, TX 79409-1061, USA*

[c] *Institute for Theoretical Chemistry, University of Vienna, Währingerstr. 17, A-1090 Vienna, Austria*

*Corresponding Authors: Mario Barbatti – barbatti@kofo.mpg.de; Hans Lischka – hans.lischka@univie.ac.at

Abstract

2-Aminopurine (2AP) is often chosen as a fluorescent replacement for purine bases and used as a probe in nucleic acid research. The luminescence of this molecule is strongly dependent on the environment. Through computational simulations of isolated 2AP and a series of 2AP-water clusters, we show that the experimentally-observed dependence of the excited-state lifetime of 2AP on the number and location of water molecules is controlled by a barrier for internal conversion between the S_1 minimum and a conical intersection. Other possible competing pathways (proton transfer, intersystem crossing, and internal conversion at other intersections) were also investigated but discarded. The tuning of the luminescence of 2AP by water is related to the order of the $n\pi^*$ and $\pi\pi^*$ states. When a water molecule interacts with the amino group, the pathway from the S_1 minimum to the conical intersection requires a nonadiabatic change, thus raising the energy barrier for internal conversion. As a consequence, a single water molecule hydrogen-bonded to the amino group is sufficient to make 2AP fluorescent.

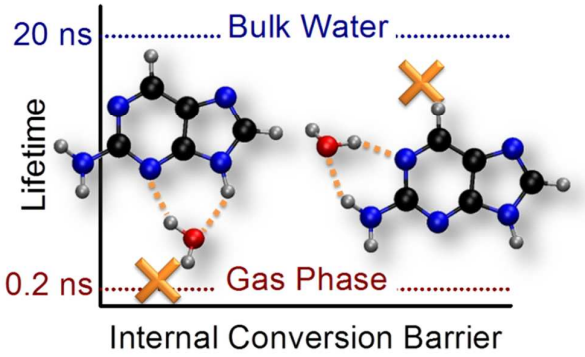

1 INTRODUCTION

In the last two decades a major paradigm shift has taken place in viewing photophysical processes. Until the late 1990s, excited-state processes were commonly analyzed in terms of diverse phenomenological models, as the Lim proximity model for fluorescence quenching,[1] the El-Sayed rules for intersystem crossing,[2] or the many formulas (Landau-Zener, Rosen-Zener, Delos-Thorson, etc.) for nonadiabatic transition probabilities.[1-4] This type of analysis has been mostly replaced by mechanistic investigations based on static and dynamic exploration of reaction pathways connecting stationary points and conical intersections.[5-7] The main goal of the mechanistic approach is to provide a unique framework, with a reduced and generally valid number of concepts, to analyze different phenomena and molecular systems. The mechanistic approach does not aim at proving former phenomenological models wrong, but rather tries to incorporate them as particular cases adapted to specific situations.

Greatly motivated by the development of new methods well adapted to the modern computational capabilities, the mechanistic approach has been applied to a large number of different molecular systems.[6] Nevertheless, a recent publication,[8] reporting a state-of-the-art time-resolved spectroscopy of microsolvated 2-Aminopurine (2AP), has challenged the mechanistic approach, by showing that a particular phenomenological model could provide a better rationale for those experiments than the analysis of excited-state reaction pathways to the conical intersections available up to now. In this paper, we are taking up the challenge of showing that the mechanistic approach can properly explain the photophysics induced by microsolvation of 2AP.

Due to its similarity to adenine and guanine, 2AP (Fig. 1), has been often used as a fluorescence probe for nucleic acid structure and dynamics.[9] However, the luminescence of 2AP is strongly depedent on the environment.[10] It is intense in protic environments (water, ethanol, tetrafluoroethylne[11]) and moderate in covalently bonded 2AP-nucleobase dimers.[12] It is weak in nonpolar solvents (dioxane[10, 11]), polar aprotic solvents (dimethylformamide[11]), nucleic acid strands,[13] and in the gas phase.[14]

Isolated in the gas phase, it takes 156 ps for 2AP to return to the ground state after excitation at the 0_0^0 band (309 nm).[8] This time reduces to 88 ps at 295 nm (Supporting Information of Ref.[8]) and to 30 ps at 267 nm.[15] The sharp lifetime decrease is an indication that shorter wavelengths are triggering internal conversion, although an inefficient one: for comparison, gas phase adenine excited at the same 267 nm has a lifetime of only 1 ps.[15]

Internal conversion, however, does not tell the full story of 2AP deactivation in the gas phase. After excitation at the 0_0^0 band, a dark triplet state with 5-μs lifetime is supposed to be populated.[14, 16] Thus, at least for 0_0^0 excitation, internal conversion and intersystem crossing may be competing with each other.

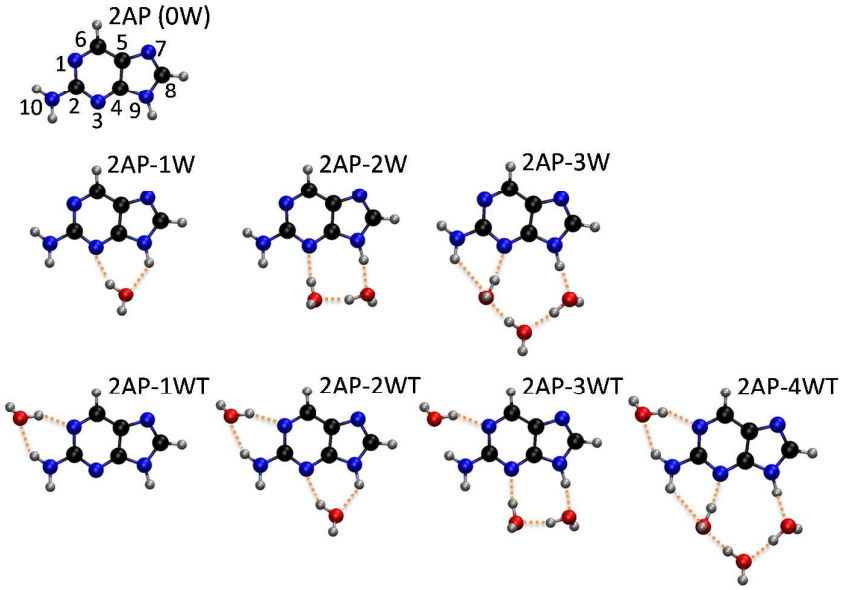

Fig. 1. Ground state geometries of 2AP (9H-2-aminopurine) and of 2AP-water clusters.

Dissolved in water, 2AP becomes a fluorescent species with a lifetime of τ_F = 11.8 ns and a quantum yield of Φ_F = 0.66, corresponding to a natural lifetime (τ_F/Φ_F) of 17.9 ns.[17] Time-resolved spectroscopy of microsolvated 2AP has revealed[8] that already a single water molecule hydrogen-bonded to the amino group is enough to raise the lifetime by two orders of magnitude in comparison to that in the in the gas phase. Together with quantum chemical calculations, this set of experiments[14] made clear that the lifetime increase is correlated to the simultaneous stabilization of the ππ* state and destabilization of the nπ* state induced by the water molecules.

Based on quantum chemical modeling in the gas phase, a number of authors[18-20] have proposed that fluorescence in 2AP occurs because the conical intersections with the ground state, created by strong out-of-plane distortions of the pyrimidine ring either around C6 or around C2 (Fig. 1), are separated from the excited-state minimum by significant energy barriers. Lobsiger and co-workers[8] have criticized such explanation on the grounds that these barriers, already present in the gas phase, would imply that isolated 2AP is fluorescent, in contradiction with the experimental measurements. They then resorted to the Lim proximity model[1] to explain the experimentally observed correlation between the cluster size and the excited-state lifetime.

Stated in terms of the current problem, the Lim proximity model[1] predicts that the internal conversion rate from the first excited state to the ground state is enhanced when there is a small energy gap between the ππ* and the nπ* states at the Franck-Condon point, due to the strong vibronic coupling between these states along an out-of-plane vibrational mode.[21] Thus, the stabilization of the

ππ* state and destabilization of the nπ* state induced by the water molecules would increase the gap, reduce the coupling, reduce the internal conversion rate, and turn 2AP fluorescent.

In this work, our aim is to use computational simulations to understand how water influences the excited-state relaxation of 2AP from a mechanistic point of view. The questions we want to address are, first, how does water tune the excited states in the way we just described? Second, what is the relative importance of the multiple relaxation and isomerization mechanisms (internal conversion, proton transfer, intersystem crossing) as a function of the solvent and of the excitation energy? Finally, what are the factors behind the empirical correlation between cluster size and lifetime?

Inspired by the microsolvation experiments,[8] we systematicaly studied 2AP isolated and in clusters with up to four water molecules (Fig. 1). For each of the total of eight species, we characterized minima in the ground and in the excited states, energy gaps for intersystem crossing, conical intersections for internal conversion to the ground state, and excited-state transition barriers for accessing these intersections and also to undergo intramolecular proton transfer. The patterns that emerged from a comparative analysis of these properties through the series of clusters show that the mechanistic analysis of the reaction paths to the conical intersections provides a complete justification of the experimental findings.

2 COMPUTATIONAL DETAILS

The excited-state calculations were performed with the algebraic diagrammatic construction to second order (ADC(2))[22, 23] and the second-order approximate coupled cluster (CC2),[24-26] both using the resolution of the identity (RI) approximation as implemented in Turbomole.[27] For ADC(2) excitations, the reference ground state was computed with the second-order Møller-Plesset perturbation theory (MP2).[25] The aug-cc-pVDZ basis set[28] was adopted for all calculations. Transition states in the excited state were optimized with the Trust Radius Image Minimization method (TRIM)[29] as implemented in Turbomole. Hessians were computed numerically and recomputed after optimization. Conical intersections (within 0.02 eV) were optimized with the penalty Lagrange multiplier technique (α = 0.02 hartree) implemented in the CIOPT program,[30] which we have adapted to work with ADC(2) and Turbomole.

The formalism for computing ADC(2) excitation energies, which was originally derived using diagrammatic perturbation theory, [22] may be expressed as the eigenvalues of a symmetrized Jacobian of a coupled cluster method with perturbative-doubles correction.[31] It has errors similar to those of CC2[32] at reduced computational costs. The symmetric Jacobian in ADC(2) increases the numerical stability of this method in the case of quasi-degenerate excited states.

Recent investigations on internal conversion of adenine in the gas phase[33] and in water clusters,[34] of exciplex formation in adenine dinucleotide,[35] and of excited-state intramolecular proton transfer in

7-azaindole in water clusters[36] have shown that the ADC(2) method is a useful and efficient tool to reliably compute excited-state energy surfaces for the purpose of the photo-deactivation dynamics of nucleobases. In spite of the fact that it is a single-reference method, even the intersection regions between S_1 and S_0 can be successfully investigated using ADC(2) as a comparison of computed adenine decay times with experimental data and diverse other simulation methods has shown.[33]

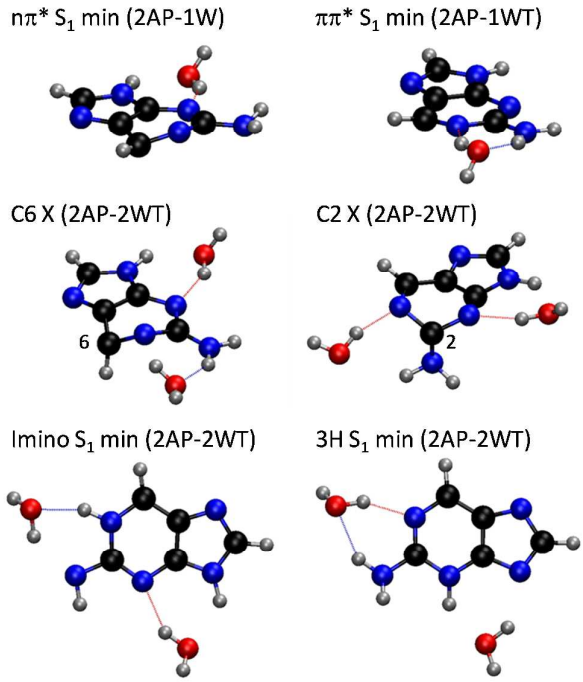

Fig. 2. Geometries of the S_1 minima (nπ* for 2AP-1W and ππ* for 2AP-1WT), of the conical intersections (C6 X and C2 X for 2AP-2WT), and of the S_1 minima after proton transfer (imino and 3H for 2AP-2WT).

3 RESULTS

3.1 Ground and Excited-State Minima

The 9H tautomer of 2AP is strongly dominant in the gas phase.[20, 37] For this reason, all our simulations were based on it. Several cluster models containing up to four water molecules were built, following the cluster assignment given in previous experimental microsolvation studies.[8, 38, 39] Two clusters of 2AP with one water molecule each were chosen. In the first one, denoted 2AP-1W, the water is near N3 and N9 (Fig. 1). In the other (2AP-1WT), the water is near N1 and N10. (T in WT notation indicates a water at the trans-amino site.) A third cluster with one water near N7 was also built, but since the main results for excited-state barriers for it were very similar to those obtained for 2AP-1W, this third cluster will not be further discussed. Two clusters with two water molecules were

built, 2AP-2W (water molecules near N3 and N9) and 2AP-2WT (one water near N3-N9, another water near N1 and N10). Following the same pattern and notation, two clusters with 3 water molecules, 2AP-3W and 2AP-3WT, were built. Finally, the cluster 2AP-4WT containing four water molecules was built. At the end, 8 species were investigated, isolated 2AP (0W), three clusters in the W series (1W, 2W, 3W), and four clusters in the WT series (1WT, 2WT, 3WT, 4WT). With the exception of 2AP-4WT, there are experimental data[8] and theoretical (TDDFT, CC2)[38] vertical and adiabatic excitation energies available for all other clusters.

Table 1 – Vertical excitation (ΔE_v), adiabatic excitation (ΔE_a), vertical emission (ΔE_e), oscillator strengths (f), and state character for all studied species. Absorption was computed at the S_0 minimum. Adiabatic excitation and emission were computed at the S_1 minimum of the 9H tautomer.

	S_0 minimum			S_1 minima			
Geometry	State	ΔE_v (eV)	f	State	ΔE_a (eV)	ΔE_e (eV)	f
2AP	ππ*	4.32	0.155	nπ*	3.89	2.99	0.006
				ππ*	3.93	3.14	0.098
2AP-1W	ππ*	4.31	0.165	nπ*	3.93	2.75	0.022
				ππ*	3.93	3.37	0.135
2AP-2W	ππ*	4.28	0.167	ππ*	3.90	3.49	0.148
				nπ*	3.92	2.73	0.035
2AP-3W	ππ*	4.25	0.163	ππ*	3.85	3.25	0.127
2AP-1WT	ππ*	4.17	0.146	ππ*	3.80	3.33	0.122
2AP-2WT	ππ*	4.17	0.157	ππ*	3.79	3.37	0.136
2AP-3WT	ππ*	4.12	0.159	ππ*	3.76	3.29	0.133
2AP-4WT	ππ*	4.10	0.155	ππ*	3.73	3.23	0.126

The geometries of the ground state (S_0) and of the first excited state (S_1) were optimized for all clusters (Cartesian Coordinates are given in the Supporting Information). The vertical excitation, adiabatic excitation, vertical emission, and oscillator strengths are given in Table 1. Characterization of these higher excited states in terms of single-excitation contributions are provided in the Supporting Information, Section S1.

A comparison of vertical excitations computed with different methods is given in Table S3 of the Supporting Information. The most complete series of data available among the previous publications are the TD-B3LYP/TZVP results of Lobsiger et al. (Supporting Information of Ref.[8]). In that work, excitations for all clusters up to 2AP-3WT are reported. These TD-B3LYP and our ADC(2) results are in excellent agreement. The mean root-mean-square deviation (RMSD) including 19 transitions is 0.1 eV for energies and 0.09 for oscillator strengths. The ADC(2) results, however, additionally provide information about Rydberg states, which is missing in the TDDFT benchmark. DFT/MRCI results[20] are available only for 2AP. Again, the energies (including a Rydberg state) and oscillator strengths compare well to those obtained with ADC(2). Vertical excitations for 2AP are also available with CASPT2.[19] The energies (only valence states) are in good agreement with ADC(2) energies. The oscillator strengths of the first and second ππ* transitions are switched, with CASPT2 being in

disagreement with the other three methods. The CASPT2 oscillator strengths also show strong basis set dependence, as discussed in the Supporting Information of Ref.[19].

For 2AP and all clusters, the S_1 state at the ground state minimum is a bright ππ* transition. The S_1 minimum, however, can have nπ* or ππ* character for 2AP, 2AP-1W, and 2AP-2W, while it is only ππ* for 2AP-3W and for the whole WT series. The nπ* S_1 minima are puckered at N1 (as shown in Fig. 2 for 1W), while the ππ* S_1 minima are less distorted (Fig. 2 shows it for 1WT). These S_1 minima will be referred to as 9H S_1 minima whenever there is risk of mistaking them for other minima obtained upon proton transfer.

For 2AP (0W), ADC(2) predicts a ππ* S_1 minimum slightly above the nπ* S_1 minimum by 0.04 eV. A linearly-interpolated energy profile shows that the ππ* state is separated from the nπ* state by a barrier smaller than 0.02 eV, which means that even after an excitation at the ππ* origin, the nπ* can be easily populated via tunneling. The relative position of the nπ* and ππ* minima is in agreement with CC2,[16] TDDFT,[16] and DFT-MRCI//TDDFT[20] results. CASPT2//CASSCF[19] and CASSCF[18] also predict a quasi-degeneracy between these two states, but with the ππ* minimum slightly lower by ~0.1 eV. The CASPT2//CASSCF results from Ref.[18] do not fit into this picture and place the ππ* state 0.64 eV lower than the nπ*. Excepting this last result, all other nπ*–ππ* energy gaps are within the uncertainty of any excited-state method (0.1-0.2 eV),[32] meaning that it is not possible to computationally establish the order of the nπ* and ππ* states at this time.

With the sequential addition of water, the nπ* state is destabilized in such a way that the nπ* and ππ* S_1 minima are degenerate already for 2AP-1W (Table 1). The nπ* S_1 minimum is slightly above the ππ* S_1 minimum for 2AP-2W and for the remaining clusters the nπ* minimum is already S_2. For 2AP and the WT series, the S_1 state assignment in Table 1 is the same as that from TD-B3LYP/TZVP calculations reported in Ref.[8]. There are small divergences in the W series, but always within the accuracy of the computational methods. Concerning the 2AP-1W and 2AP-1WT clusters, resonant two-photon ionization (R2PI) spectroscopy[39] shows a coupling of the optically active ππ* state to a lower-lying nπ* state for 2AP-1W but not for 2AP-1WT. This is an indication that the nπ* should dominate the S_1 state in 2AP-1W, while the ππ* state should do it in 2AP-1WT. For this reason, when discussing the emission properties of 2AP-1W, we take the nπ* minimum as the reference.

3.2 Paths for Excited-State Relaxation

From the S_1 minimum (Fig. 2), we have considered the following possible excited-state reaction processes occurring after an UV excitation:

1) internal conversion at C6-puckered conical intersection;

2) internal conversion at C2-puckered conical intersection;

3) proton transfer from N9 to N3 through the water bridge, forming the 3H tautomer;

4) proton transfer from N10 to N1 through the water bridge, forming the imino tautomer;

5) intersystem crossing to triplet states.

For computing the internal conversion pathways, conical intersections either puckered at C6 or at C2 were optimized for 2AP and all clusters (see Supporting Information for Cartesian Coordinates). These conical intersections are illustrated in Fig. 2 for 2WT. For computing the proton-transfer paths, the S_1 minimum of the 3H and the imino tautomers were also optimized (also shown in Fig. 2 for 2WT). Finally, transition states in the S_1 state were optimized a) between the 9H S_1 minimum and the two conical intersections and b) between the 9H S_1 minimum and the S_1 minima of the proton-transferred tautomers.

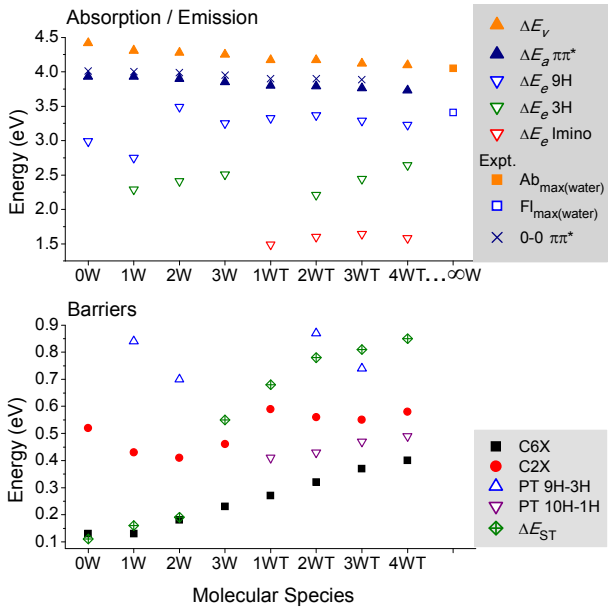

Fig. 3. (Top) Vertical excitation (ΔE_v), adiabatic excitation (ΔE_a), and vertical emission (ΔE_e) energies for all species. Vertical excitations into the S_1 state (ππ*). Emission from the lowest 9H S_1 minimum (nπ* for 0W and 1W; ππ* for the others) and from the S_1 minima after proton transfer to N3 (3H) or N1 (1H). Experimental absorption and emission in aqueous solution from Ref.[17]. Experimental 0_0^0 ππ* excitations for 2AP and 2AP-water clusters from Ref.[8]. (Bottom) Energy barriers from the (9H) S_1 minimum to reach the conical intersections (C2 X and C6 X) and from that minimum to reach the S_1 minima of the 3H and 1H tautomers. ΔE_{ST} is the energy gap between T_2 and S_0. Tables with all energy values are given in the Supporting Information (Sections S1, S2, and S3); see also Table 1.

Fig. 3-top shows the vertical (ΔE_v) and adiabatic (ΔE_a) excitation energies and the vertical emission energies (ΔE_e) from 9H, 3H, and imino (1H) S_1 minima for all species. Experimental ππ*

origins,[8] as well as absorption and emission energies of 2AP in bulk water are also displayed.[17] The presence of water near the amino group in the WT series has a very strong impact, rendering computed vertical excitation and fluorescence energies near to the bulk water even for the smallest cluster (2AP-1WT). It is also clear that the 2AP emission in water occurs mainly from the 9H tautomer.

Fig. 3-bottom shows the excited-state energy barriers to the conical intersections. These values imply that internal conversion at C6 intersection is accessible for 2AP, 2AP-1W, and 2AP-2W even at low excitation energies. The barrier increases systematically blocking this path for WT clusters. Internal conversion at the C2 intersection has larger barriers between 0.4 and 0.6 eV, with no distinguishable correlation with the cluster size.

Barriers for excited-state intramolecular proton transfer from N10 to N1 forming the imino tautomer are between 0.4 and 0.5 eV. They systematically increase along the WT series. These barriers lie between the barriers for internal conversion at C2 and at C6 intersections. Barriers for proton transfer from N9 to N3 are even larger, above 0.7 eV.

Fig. 3-bottom also shows the T_2-S_1 energy gap to activate intersystem crossing computed from the S_1 minimum. T_2 was chosen because, for all species, it is the triplet state lying the closest to S_1 with favorable intersystem crossing according to the El-Sayed's rule.[2, 40] (The El-Sayed's rule states that the rate of intersystem crossing is larger for transitions involving a change of molecular orbitals type, than for transitions between the same orbital types.) For isolated 2AP, intersystem crossing from S_1 ($^1n\pi^*$) to T_1 ($^3n\pi^*$) is unfavorable (see Supporting Information Section S3). Nevertheless, it may occur to the T_2 state ($^3\pi\pi^*$). Intersystem crossing should also be possible between S_1 ($^1n\pi^*$) and T_1 or T_2 (both are $^3\pi\pi^*$) for 2AP-1W and 2AP-2W. For 2AP-3W and all WT clusters, the large energy gaps above 0.5 eV should make this process improbable. These results are consistent with the relatively large phosphorescence quantum yield of 2AP in an aprotic solvent (0.14 in ether) and the small phosphorescence quantum yield in a protic solvent (0.02 in ethanol).[41]

4 DISCUSSION

According to the time-resolved microsolvation experiments,[8] after UV-excitation at the 0_0^0 band, the excited-state lifetime increases systematically with the cluster size and water position. This means that there is at least one nonradiative path competing with fluorescence and that the probability of activating this path is decreasing with the increasing of the cluster size. Among all five relaxation paths that we have considered in the previous section (see Fig. 3-bottom), only internal conversion at the C6 intersection shows a pattern that can explain this effect.

In Fig. 4, the measured excited-state lifetime[8] is plotted as a function of the computed energy barrier between the S_1 minimum and the C6 intersection. It shows a nice correlation along the sequence of clusters, with larger lifetimes corresponding to higher energy barriers. The lifetimes

plotted in this way approach asymptotically the experimental natural lifetime in bulk water (17.9 ns).[17] This comparison shows that not only the properties at the S_1 minimum (energy gap and order of nπ* vs. ππ* states),[8] but also the energy barriers to the conical intersections as a measure of the dynamical properties correlate well with the experimental lifetimes.

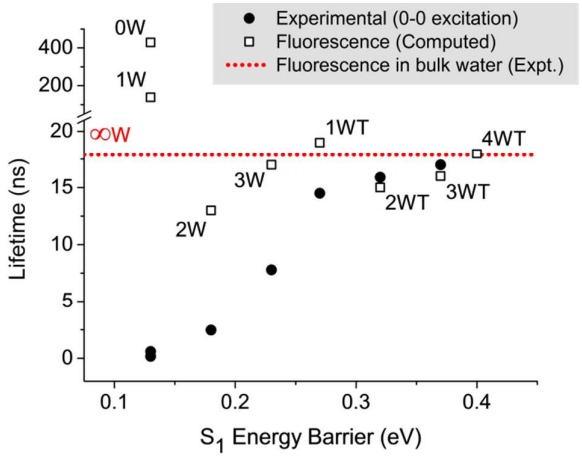

Fig. 4. Experimental excited-state lifetime after 0_0^0 excitation[8] as a function of the computed energy barrier for reaching C6 X from the S_1 minimum. Experimental natural lifetime of 2AP in bulk water[17] and estimated radiative lifetime are also shown.

In Fig. 4, the estimated radiative lifetimes are also shown (see also Table S2 in the Supporting Information). In atomic units, they are given by

$$\tau_{rad} = -\frac{1}{2}\frac{c^3}{f\Delta E_e^2} \qquad (1)$$

where c is the speed of light, f is the oscillator strength, and ΔE_e is the emission energy gap (Table 1). The series starts with very large τ_{rad}, but it quickly converges to the bulk water result. The abrupt change in the radiative lifetime from 2AP-1W (138 ns) to 2AP-2W (13 ns) is due to the change of character of the S_1 state from nπ* to ππ* (see Table 1). Although the shift to larger energy gaps at the ππ* state also contributes to τ_{rad} reduction, the main responsible factor for it is the strong increase of f.

The deviation between the experimental lifetime and the estimated radiative lifetime in Fig. 4 tells how important the nonradiative path is. The very large deviation for isolated 2AP (0W), for instance, indicates that this species mainly relaxes via a nonradiative path, which, for this specific case, can be either the internal conversion at C6 intersection or intersystem crossing to T_2.[14, 16] The deviation between the estimated radiative lifetime and the actual lifetime is very small for all WT clusters, implying that the presence of a water molecule near the amino group makes these clusters fluorescent.

The role of the water molecule near the amino group can be qualitatively understood by the stabilization of the n orbital when a water molecule is placed near the amino group in the 2AP-1WT system. This stabilization is expected as the n orbital donates electron density to the hydrogen bond. (Molecular orbitals are depicted in Fig. S4 of the Supporting Information.) In the case of 2AP-1W, the stabilization of the n orbital is less pronounced because the large N3-C4-N9 angle (~130°) does not favor a water bridge, as the N1-C2-N10 (~115°) does in case of the 2AP-1WT. As a consequence, the electronic states in 2AP-1W (also in 2W) still resemble those from isolated 2AP, with S_1 split between nπ* and ππ* characters.

2AP-3W is a special case. Although it is not in the WT series, the bridge with three water molecules pulls the water bonded to N3 towards the amino group (see Fig. 1). For the S_1 minimum, the N10-H···OH_2 distance is only 2.25 Å. For this reason, just like in the WT clusters, the energy of the nπ* state is destabilized, the S_1 has only ππ* character, and τ_{rad} is short.

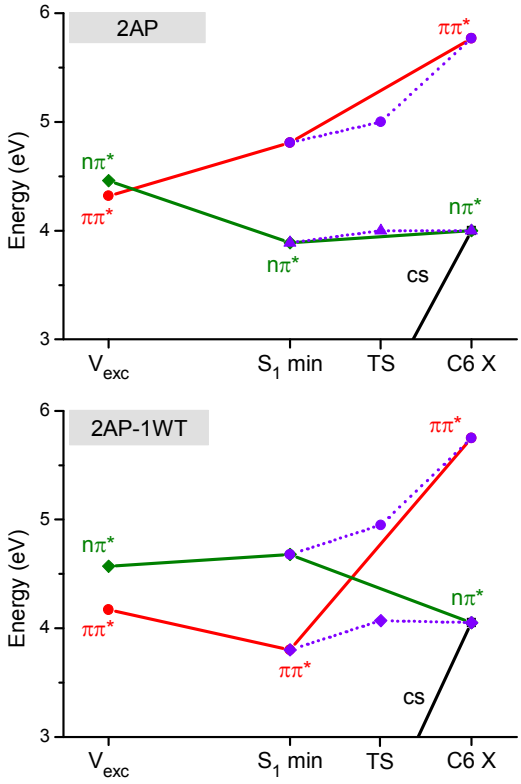

Fig. 5. Diabatic connection (full lines) of the excited-state energies at the S_0 minimum (V_{exc}), the S_1 minimum, and C6 X for 2AP (top) and 2AP-1WT (bottom). Dotted lines indicate the adiabatic connections through the S_1 transition state (TS). Electronic density differences for 2AP-1WT path are shown in Fig. S1 of the Supporting Information.

In Ref.[21], it is claimed that the cause of the destabilization of the nπ* state is the effect of the bulk water, not of the hydrogen bonds. The present results, however, make clear that the direct interaction between water and the amino group is fundamental for destabilization of the nπ* state.

The ππ* character of the S_1 state in the WT series causes a dramatic rearrangement of the potential energy profile compared to that in isolated 2AP, as shown in Fig. 5. In isolated 2AP (0W), assuming that the initial ππ* population relaxes to the nπ* state, the S_1 minimum is connected to the C6 conical intersection by an adiabatic path. The higher energy of the intersection as compared to the S_1 minimum, however, makes the internal conversion inefficient, explaining why the lifetime of 2AP is 30 times longer (at 267 nm)[15] than of the 9H-adenine, whose intersection is energetically lower than the S_1 minimum.[33] This picture is qualitatively the same for 2AP-1W and 2AP-2W, although it is complicated by the degeneracy between ππ* and nπ*. As the nπ* fraction of the wavepacket follows the internal conversion path, the ππ* fraction converts to the nπ* section of the S_1 surface to undergo the same decay process as the original nπ* state. In 2AP-3W and in the WT series, on the other hand, because of the interaction of water with the amino group, the S_1 state has ππ* character. In these cases, reaching the conical intersection requires a nonadiabatic change (avoided crossing) from ππ* into nπ* along the reaction path (Fig. 5-bottom). This change is associated with a significant barrier that tends to increase with the size of the WT cluster, favoring radiative decay over internal conversion. In the case of excitations near the band origin, the competition between internal conversion and radiative decay is essentially the same, but the internal conversion should take place when the molecule reaches regions of enhanced nonadiabatic coupling with the ground state during out-of-plane vibrations on the nπ* surface.

In this regard, this mechanistic interpretation and the Lim's proximity effect are qualitatively in agreement, as the latter also predicts that the internal conversion to the ground state takes place near the S_1/S_0 crossing induced by the S_1/S_2 coupling occurring along out-of-plane vibrations.[1] The main difference is that while the Lim's model reaches at this conclusion based on phenomenological assumptions for the shape of the potential energy surfaces, the mechanistic approach is based on the actual shape of the surfaces, as predicted by the simulations.

As mentioned in the previous section, the CASPT2//CASSCF results from Ref.[19] placed the ππ* S_1 minimum slightly below the nπ* minimum for isolated 2AP. As a consequence, the analysis of the reaction pathways in that work favored deactivation at the C2 intersection whereas our calculations show a preference for deactivation at the C6 intersection. Although we cannot clearly identify the exact reason for the divergence, the balance of the ADC(2) method toward taking into account all lone pair orbitals on equal footing and the consistency of the present results with the experiments through the whole series of clusters strongly supports the C6 intersection as the actual gate for internal conversion.

The difference between the adiabatic path in 2AP (0W) and the nonadiabatic path in the WT series can also be displayed by electron density difference plots between the excited and the ground states, as those in Fig. 6. In this figure, orange regions are electron deficient, while green regions are electron rich. Note how the density differences at the nπ* S_1 minimum and at the C6 intersection are similar, while the density difference at the ππ* S_1 minimum and at the C6 intersection are completely distinct.

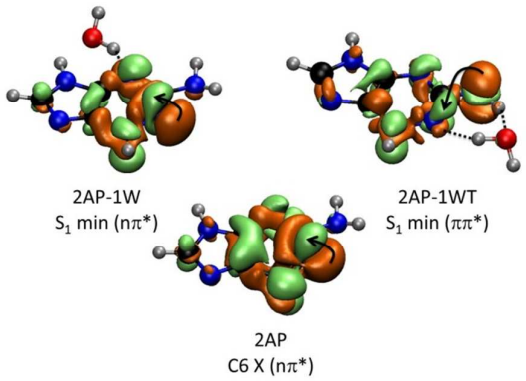

Fig. 6. S_1–S_0 electron density difference for the S_1 minimum of 2AP-1W and 2AP-1WT and at the C6 X of 2AP. Orange regions are electron donor and green regions are electron acceptor.

Incidentally, the density differences in Fig. 6 also reveal an interesting feature about the ππ* state: it has a pronounced charge-transfer character with an electron shift from the amino group to the pyrimidine ring. This feature has been experimentally described long ago,[41] but it has not been further discussed in more recent literature.

5 CONCLUSIONS

2AP shows a drastic change in the excited-state lifetime from 30 to 18000 ps when the environment is changed from the gas phase to water.[15, 17] There are two types of nonadiabatic interaction approaches in discussion to explain this phenomenon. The first approach, advocated in Ref.[8], relies on the Lim proximity model.[1] It predicts that the nonadiabatic interaction concentrates on the region of the S_1 minimum and invokes vibronic coupling via out-of-plane modes facilitating the internal conversion process to the ground state, depending on the separation between the nπ* and ππ* states ($\Delta E_{n\pi\text{-}\pi\pi^*}$). The good correlation between the calculated $\Delta E_{n\pi\text{-}\pi\pi^*}$ and the measured lifetimes has been taken as corroboration to this first approach.

The second approach is based on the analysis of the reaction path mechanisms from the Franck-Condon region to conical intersections including reaction barriers.[18, 19, 40] Although this *mechanistic*

approach should be preferred over the first one, as it relies on a global understanding of the topography of the electronic potential energy surfaces, it has been limited so far to gas-phase analysis, providing only qualitative insights on the situation in water.

In the present work, we take one step further in the mechanistic approach to provide a comprehensive analysis of the topography of the excited states of 2AP-water clusters. In particular, through computational simulations of a series of 2AP-water clusters, we show that:

1) The increase in the excited-state lifetime observed experimentally in these clusters is due to the increase of the barrier to internal conversion at a C6-puckered conical intersection. Four other possible competing pathways (internal conversion in another conical intersection, two types of proton transfer, intersystem crossing) were also considered but not found relevant.

2) The pathway to the C6-puckered conical intersection is qualitatively different starting from an nπ* or ππ* S_1 state. From nπ*, the pathway is adiabatic with small or no barrier. From ππ*, the pathway requires a nonadiabatic change, creating a barrier. Thus, for the same energy, nπ* population will have shorter lifetime than ππ* population.

3) The tuning of the luminescence of 2AP by water is related to the order of the nπ* and ππ* states. When a water molecule interacts with the amino group, it stabilizes the ππ* and destabilizes the nπ* state. The change of the state ordering initiates different dynamics since under the new energetic order the pathway from the S_1 minimum to the conical intersection requires a nonadiabatic change, raising the energy barrier for internal conversion. This barrier rising, which may block the internal conversion depending on the excitation energy, elongates the excited-state lifetime and favors fluorescence.

4) In the sequence from isolated 2AP to 2AP-4WT, we can identify three different scenarios regarding the relative positions of the nπ* and ππ* states: a) the nπ* character dominates the S_1 state (0W), b) nπ* and ππ* are almost degenerate and the S_1 population should split between them (1W and 2W), and c) ππ* dominates the S_1 state (3W and WT series). The first scenario should favor internal conversion due to the small energy barriers to the conical intersection, rendering relatively short lifetimes. The last scenario, on the other hand, should favor radiative decay and long lifetimes because of large barriers. In the second scenario, internal conversion of nπ* population fed by a flow from ππ* to nπ* should grant intermediary lifetimes.

Interestingly, a comparative analysis of previous experimental results[8, 17] showed that a single water molecule hydrogen-bonded to the amino group (1WT) is enough to render a lifetime already near to that observed in bulk water. This good agreement comes from the fact that in this case the S_1 state has ππ* character, and as such, not only internal conversion is blocked as discussed above, but also the radiative lifetime is strongly shortened by the large oscillator strength of this state as opposed to the cases where the water molecules are located in other positions (W series) and the S_1 state has

nπ* character. Notwithstanding this nice agreement, it is clear that for a complete description of the fluorescence properties in aqueous solution much more than one water molecule is needed.

Taken together, the results reported in this work indicate that the correlation between the excited-state lifetime and $\Delta E_{n\pi-\pi\pi^*}$ observed in Ref.[8], rather than simply corroborating the Lim proximity model, reflects a topographic feature of the potential energy surfaces – the barriers between the excited-state minima and the conical intersections – which ultimately controls the internal conversion rate.

ASSOCIATED CONTENT

Electronic Supplementary Information (ESI) available: Characterization of vertical states up to S_4, comparison to previous results, characterization of the S_1 minima, energies of stationary points and conical intersections, electronic density differences along the reaction path for C6 X, characterization of the triplet states, molecular orbitals, Cartesian coordinates. See DOI: 10.1039/b000000x/

ACKNOWLEDGEMENT

This work was supported by the National Science Foundation under Project No. CHE-1213263 and the Robert A. Welch Foundation under Grant No. D-0005.

REFERENCES

1 E. C. Lim, *J. Phys. Chem.*, 1986, **90**, 6770.

2 M. A. El-Sayed, *J. Chem. Phys.*, 1963, **38**, 2834.

3 M. Desouter-Lecomte and J. C. Lorquet, *J. Chem. Phys.*, 1979, **71**, 4391.

4 J. Michl and V. Bonačić-Koutecký, *Electronic Aspects of Organic Photochemistry*, Wiley-Interscience, 1990.

5 W. Domcke, D. R. Yarkony and H. Köppel, *Conical Intersections - Electronic Structure, Dynamics and Spectroscopy*, World Scientific, Singapore, 2004.

6 W. Domcke, D. R. Yarkony and H. Köppel, *Conical Intersections - Theory, Computation and Experiment*, World Scientific, Singapore, 2011.

7 F. Bernardi, M. Olivucci and M. A. Robb, *Chem. Soc. Rev.*, 1996, **25**, 321.

8 S. Lobsiger, S. Blaser, R. K. Sinha, H.-M. Frey and S. Leutwyler, *Nat Chem*, 2014, **6**, 989.

9 R. W. Sinkeldam, N. J. Greco and Y. Tor, *Chem. Rev.*, 2010, **110**, 2579.

10 S. Bharill, P. Sarkar, J. D. Ballin, I. Gryczynski, G. M. Wilson and Z. Gryczynski, *Anal. Biochem.*, 2008, **377**, 141.

11 E. L. Rachofsky, R. Osman and J. B. A. Ross, *Biochemistry*, 2001, **40**, 946.

12 C. Wan, T. Xia, H.-C. Becker and A. H. Zewail, *Chem. Phys. Lett.*, 2005, **412**, 158.

13 J. M. Jean and K. B. Hall, *Proc. Natl. Acad. Sci. USA*, 2001, **98**, 37.

14 K. Feng, G. Engler, K. Seefeld and K. Kleinermanns, *ChemPhysChem*, 2009, **10**, 886.

15 C. Canuel, M. Mons, F. Piuzzi, B. Tardivel, I. Dimicoli and M. Elhanine, *J. Chem. Phys.*, 2005, **122**, 074316.

16 S. Lobsiger, R. K. Sinha, M. Trachsel and S. Leutwyler, *J. Chem. Phys.*, 2011, **134**, 114307.

17 A. Holmén, B. Nordén and B. Albinsson, *J. Am. Chem. Soc.*, 1997, **119**, 3114.

18 S. Perun, A. L. Sobolewski and W. Domcke, *Mol. Phys.*, 2006, **104**, 1113.

19 L. Serrano-Andrés, M. Merchán and A. C. Borin, *Proc. Natl. Acad. Sci. USA*, 2006, **103**, 8691.

20 K. A. Seefeld, C. Plutzer, D. Lowenich, T. Haber, R. Linder, K. Kleinermanns, J. Tatchen and C. M. Marian, *Phys. Chem. Chem. Phys.*, 2005, **7**, 3021.

21 E. L. Rachofsky, J. B. A. Ross, M. Krauss and R. Osman, *J. Phys. Chem. A*, 2001, **105**, 190.

22 J. Schirmer, *Phys. Rev. A*, 1982, **26**, 2395.

23 A. B. Trofimov and J. Schirmer, *J. Phys. B: At., Mol. Opt. Phys.*, 1995, **28**, 2299.

24 O. Christiansen, H. Koch and P. Jorgensen, *Chem. Phys. Lett.*, 1995, **243**, 409.

25 C. Hättig and F. Weigend, *J. Chem. Phys.*, 2000, **113**, 5154.

26 C. Hättig and A. Köhn, *J. Chem. Phys.*, 2002, **117**, 6939.

27 R. Ahlrichs, M. Bär, M. Häser, H. Horn and C. Kölmel, *Chem. Phys. Lett.*, 1989, **162**, 165.

28 T. H. Dunning, *J. Chem. Phys.*, 1989, **90**, 1007.

29 T. Helgaker, *Chem. Phys. Lett.*, 1991, **182**, 503.

30 B. G. Levine, J. D. Coe and T. J. Martínez, *J. Phys. Chem. B*, 2008, **112**, 405.

31 C. Hättig, *Adv. Quantum Chem.*, 2005, **50**, 37.

32 N. O. C. Winter, N. K. Graf, S. Leutwyler and C. Hattig, *Phys. Chem. Chem. Phys.*, 2013, **15**, 6623.

33 F. Plasser, R. Crespo-Otero, M. Pederzoli, J. Pittner, H. Lischka and M. Barbatti, *J. Chem. Theory Comput.*, 2014, **10**, 1395.

34 M. Barbatti, *J. Am. Chem. Soc.*, 2014, **136**, 10246.

35 F. Plasser and H. Lischka, *Photochemical & Photobiological Sciences*, 2013, **12**, 1440.

36 N. Kungwan, K. Kerdpol, R. Daengngern, S. Hannongbua and M. Barbatti, *Theor. Chem. Acc.*, 2014, **133**, 1.

37 R. K. Sinha, S. Lobsiger and S. Leutwyler, *J. Phys. Chem. A*, 2011, **116**, 1129.

38 S. Lobsiger, R. K. Sinha and S. Leutwyler, *J. Phys. Chem. B*, 2013, **117**, 12410.

39 R. K. Sinha, S. Lobsiger, M. Trachsel and S. Leutwyler, *J. Phys. Chem. A*, 2011, **115**, 6208.

40 C. M. Marian, *WIREs: Comp. Mol. Sci.*, 2012, **2**, 187.

41 J. Smagowicz and K. L. Wierzchowski, *J. Lumin.*, 1974, **8**, 210.